

Study and Comparative Analysis of Effect of SiC and Graphite Composite on Aluminium using RSM Methodology

Mr. Ajinkya Ramrao Yadav ,
M.E, Mechanical Engineering,
Everest College of Engineering and Technology Aurangabad.

Prof. Rahul D. Shelke,
Associate professor,
Mechanical Engineering, Everest college of Engineering
And Technology Aurangabad.

Prof. Navnath S. Kalyankar
Assistant professor,
Mechanical Engineering, Everest college of Engineering
And Technology Aurangabad.

Abstract:- In this present work, systematic study has been conducted to investigate the wear phenomenon by adding micron size silicon carbide and graphite particles into Al6061 base. Al6061 compound was taken as the base lattice to which SiC and graphite particulates were utilized as fortifications. 3 wt. %, 6 wt. %, & 9 wt. % of SiC and 3 wt. %, 6 wt. %, & 9 wt. % of graphite were introduced to the base framework. The wear behavior analysis, which uncovered the uniform appropriation of SiC and graphite content in the Al matrix. Pin on-disc equipment was utilized to assess the volumetric wear loss of arranged samples, in which EN32 steel disc was utilized as the counter face. The outcomes uncovered that the volumetric wear misfortune was expanded with increment in applied load, disc speed and sliding distance for every one of the specimens. The outcomes additionally showed that the volumetric wear loss of the Al 6061-9 % SiC-9 % graphite composite was smaller than the Al 6061-9 % SiC-9 % graphite. The worn out surfaces were portrayed by RSM analysis.

1. INTRODUCTION

1.1 Metal Matrix Composite

The metal matrix composites (MMCs) are very attractive materials for several applications. For many researches the term MMCs is often equated with the term light metal matrix composites. Substantial progress in the development of light metal matrix composites has been achieved in recent decades, so that they could be introduced into the most important applications.

Aluminum matrix composites (AMCs) are the competent material in the industrial world. Efforts have been made to develop aluminium metal matrix composites in recent years due to their low density, high strength, and superior creep resistance and have great potential in automotive and aerospace applications. Aluminium (Al) is the second most widely used metal in the world today after iron. It has a low density (2.7 g/cc), superior malleability, excellent corrosion resistance, good thermal conductivity (237 W/mK), very low electrical resistivity ($2.65 \times 10^{-8} \Omega m$) and good formability. It's Young's modulus is 70 GPa and its Vickers hardness is 60 to 70 VHN. Al has a melting point of 660.32°C and at high temperatures, the strength of Al decreases. However, the demand for Al and its alloys having a much higher strength is increasing [3].

Al matrix composites (AMCs) have been widely used in automobile and aerospace industries due to their excellent physical and mechanical properties. To overcome these shortcomings and to meet the ever increasing demand of modern day technology, composites are one of the most promising materials [3].

1.2 Alloy - Aluminium 6061

6061 (UNS designation A96061) is a precipitation-hardened aluminum alloy, containing magnesium and silicon as its major alloying elements. Originally called "Alloy 61S", it was developed in 1935. It has good mechanical properties, exhibits good weld ability, and is very commonly extruded (second in popularity only to 6063). It is one of the most common alloys of aluminum for general-purpose use. It is commonly available in pre-tempered grades such as 6061-O (annealed), tempered grades such as 6061-T6 (solutionized and artificially aged) and 6061-T651 (solutionized, stress-relieved stretched and artificially aged).

6061 Aluminum Alloy Composition by Mass %

Al	Mg	Si	Fe	Cu	Cr	Zn	Ti	Mn	Remainder
95.85 - 98.56	0.8 - 1.2	0.40 - 0.8	0.0 - 0.7	0.15 - 0.40	0.04 - 0.35	0.0 - 0.25	0.0 - 0.25	0.0 - 0.15	0.05 each, 0.15 total

Table 1: Chemical Composition of Al-6061

1.3 Reinforcement

1.3.1 Silicon Carbide (SiC)

Silicon carbide (SiC), also known as **carborundum** semiconductor, is a containing silicon and carbon. It occurs in nature as the extremely rare mineral moissanite. Synthetic SiC powder has been mass-produced since 1893 for use as an abrasive. Grains of silicon carbide can be bonded together by sintering to form very hard ceramics that are widely used in applications requiring high endurance, such as car brakes, car clutches and ceramic plates in bulletproof vests. Electronic applications of silicon carbide such as light-emitting diodes (LEDs) and detectors in early radios were first demonstrated around 1907. SiC is used in semiconductor electronics devices that operate at high temperatures or high voltages, or both. Large single crystals of silicon carbide can be grown by the Lely method and they can be cut into gems known as synthetic moissanite.

Aluminum-silicon alloys exhibit several features of tribological behavior which are similar to those of aluminum-based MMCs. Zum Gahr (1987) has summarized the effect of silicon content in Al-Si alloys in dry sliding wear. Wear resistance is improved in mild wear conditions if the silicon content in Al-Si alloys is increased. Andrews. (1985) measured mild wear of several hypereutectic Al-Si pins with approximately the same matrix composition sliding against an M2 steel disc. The wear resistance of each alloy increased with primary silicon content up to a maximum at 17% Si (total matrix and primary Si content of 26%). A transition load at which wear rates changed from mild to severe was also identified for different silicon contents and sliding speeds. Based on data from Andrews. (1985), a load-velocity diagram is plotted in that indicates the beneficial effect of silicon content on resistance to severe wear. The onset of severe wear occurred at a characteristic transition load, at which a small quantity of aluminum adhered to the steel disk. This transferred deposit grew in size and initiated gross plastic deformation and fracture of the aluminum alloy pin as the test progressed. Material removal occurred by subsurface crack propagation in a composite transfer layer of aluminum and crushed silicon particles during mild wear, and by subsurface cracking at silicon particles in the highly deformed wear zone during severe wear.

1.3.2 Graphite (Gr)

The materials are commonly used for self-lubricating plain bearings or electrical contacts. They are proprietary materials owned by the Graphite Metallizing Corp. Graphite/metal alloys take advantage of graphite's special properties: it is compared to a deck of cards: individual layers slide off the top surface easily. This phenomenon gives the material a self-lubricating ability found in no other material. Graphalloy's self-lubricating features mean the operator can eliminate grease or oil that normally evaporates, congeals, or solidifies causing premature failure. The graphite matrix can be filled with a variety of impregnates to enhance chemical, mechanical and tribological properties. The material provides a constant, low coefficient of friction rather than just a surface layer, helping to protect against catastrophic failure. Lubrication is maintained even during linear motion; lubricant is not drawn out, and dust is not pulled in. Graphalloy wear components also improve reliability during low speed operation, frequent starts and stops, and switchovers from standby to continuous running. Graphalloy bushings are available in more than 100 grades of material in any desired size or geometry, including cylindrical, with or without grooves; flange or double flange; split; and metal-backed.

2. EXPERIMENTAL SET-UP

Work Material

Al-6061 + SiC + Gr

2.1 Chemical composition of base alloy

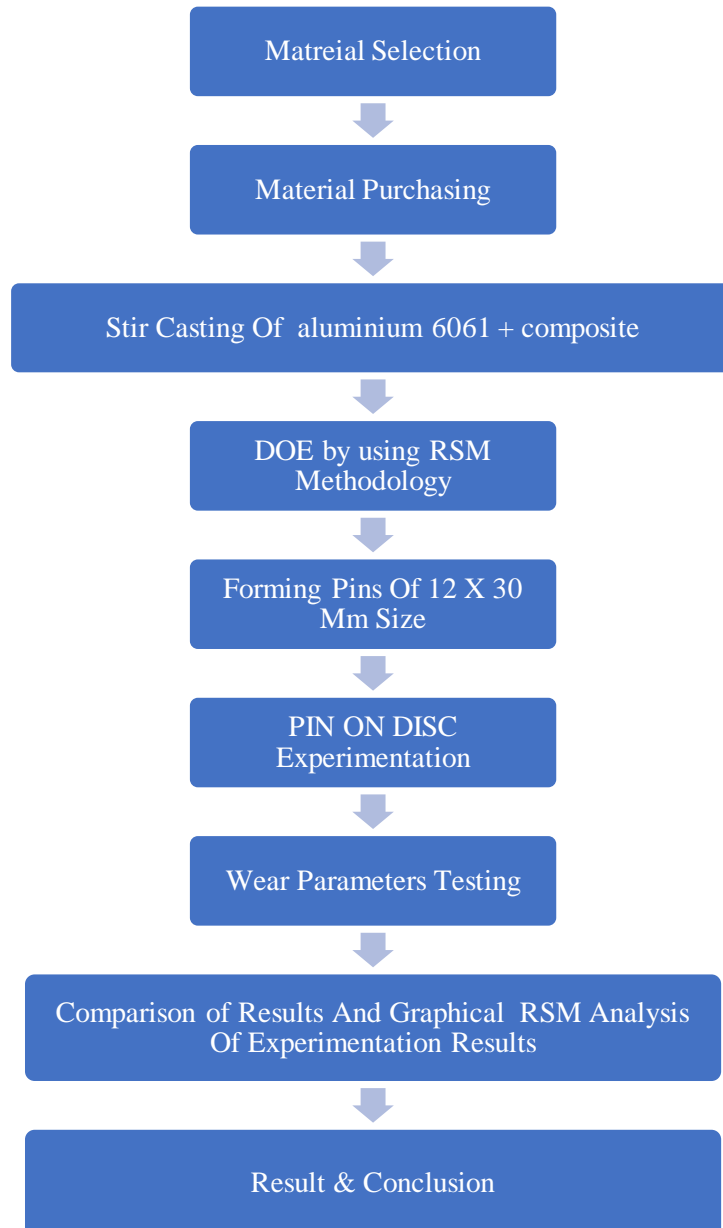
Sr. No.	Material	Minimum	Maximum
1.	Silicon	0.4%	0.8%
2.	Iron	no minimum	0.7%

3.	Copper	no minimum	0.15%
4.	Manganese	0.8%	0.4%
5.	Magnesium	0.04%	1.2%
6.	Chromium	no minimum	0.25%
7.	Zinc	no minimum	0.15%
8.	Titanium	0.05% each	0.15% total
9.	Remainder aluminium (95.85–98.56%)		

Table 2: Chemical Composition of Base Alloy

2.2 Experimental Flow chart

Fig 1: Experimental Flow Chart



2.3 Fabrication of Al MMC (AL 6061 + vol. % of SiC + Vol. % Gr) by Stir Casting

Aluminium Al6101 of commercial grade was used as the matrix material SiC and graphite particles with size varying from 26 to 30 m was used as the reinforcement material. Table 1 displays the chemical composition of Al6101 used in this research work. An orthodox casting technique was used for the manufacturing of composites. Set-up for stir casting technique is displayed in Fig. The proper amount of Al6101 was heated in a graphite crucible placed in an electric furnace. The graphite was also preheated to 720 °C with the help of a separate electric furnace. After melting the Al6101 in the electric furnace, graphite reinforcement particles (preheated) were added and mixed molten mixture was stirred at 550 rpm for 10 min by using an electric motor which is fitted with a mechanical stirrer. The temperature was kept constant (800 °C) during whole stirring.

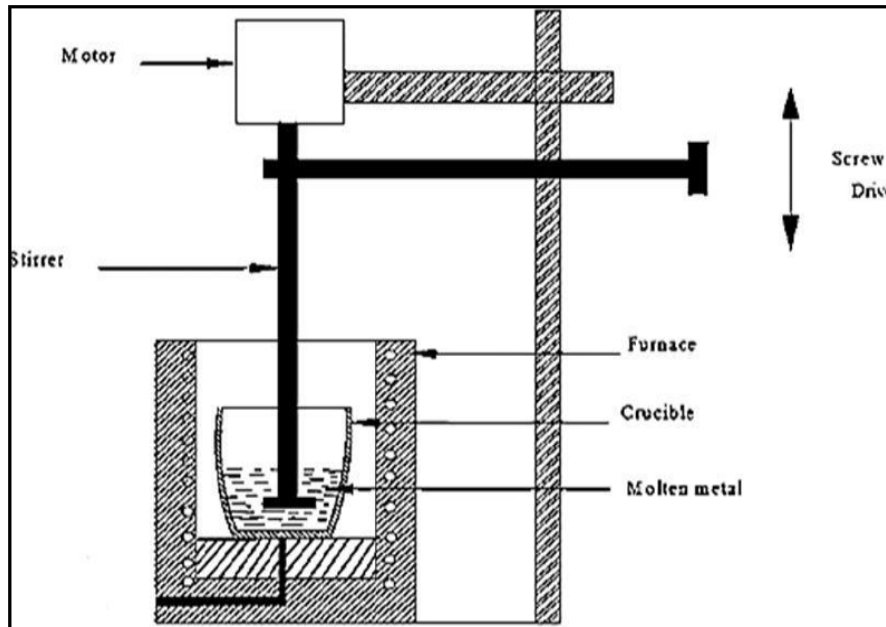


Fig 2: Stir casting machine

The molten aluminium alloy split into droplets because of shear force imparted by the stirrer at the presence of graphite. Now the molten mixture was exiled from the graphite crucible into a permanent preheated (500 °C) steel mould. The molten mixture was allowed to solidify in steel mould. The casted composite was subjected to T6 heat treatment. Heat treated composite was tested for various tests. The same procedure was followed to manufacture all other composition. The composites were manufactured at 3, 6 and 9 wt. % of SiC & graphite reinforcement particles.

3. WEAR TESTING

3.1 Technical Specification of Pin-On-Disc Machine ASTM G99 Standard.

Sr. No.	Specifications	Values
1	Disc rotation Speed	1000 rpm
2	Pin Diameter Range	ø30×12 mm
3	Disc Size (mm)	ø165×8 mm thickness
4	Sliding speed	1000 rpm
5	Wear Track Diameter	ø60×70 mm
6	Material	EN31
7	Disc hardness	58-60 HRC
8	Standard Used	G99 ASTM

Table 3: Technical Specification of Pin-On-Disc Machine

3.2 Wear testing (Pin-On-Disc Machine G99 ASTM)

The size of plate is 12 mm diameter x 700 mm, Experiment did partening of material on lathe machine the final size of material is 12 x 30 mm.

The pin was held against the counter face of a rotating disc (EN32 steel disc) with wear track diameter 80 mm. The pin was loaded against the disc through a dead weight loading system. The wear test for all specimens was conducted under the normal loads of 50N, 100N, 150N, 200N.



Fig 3: Wear Testing Setup

The pin samples were 30 mm in length and 12 mm in diameter. The samples and wear track were cleaned with acetone and weighed (up to an accuracy of 0.0001 gm. using microbalance) prior to and after each test. The wear rate was calculated from the height loss technique and expressed in terms of wear volume loss per unit sliding distance.

3.3 Procedure of Experimentation

In this study, Pin-on-Disc testing method was used for tri-biological characterization. The test procedure is as follows:

- Run-in-wear was performed in this stage. This stage avoids initial turbulent period associated with friction and wear curves. Final stage/ third stage is the actual testing called constant/ steady state wear.
- This stage is the dynamic competition between material transfer processes (transfer of material from pin onto the disc and formation of wear debris and their subsequent removal). Before the test, both the pin and disc were cleaned with ethanol soaked cotton.



Fig 4: Test Specimen

3.3.1 Weight Loss & Wear Loss

The alloy and composite samples are cleaned thoroughly with acetone. Each sample is then weighed using a digital balance having an accuracy of ± 0.1 mg. After that, the sample is mounted on the pin holder of the tribo-meter ready for wear test. The specific wear rates of the materials were obtained by

$$W = \Delta m / \rho \times L \times F$$

Where,

W denotes specific wear rates in mm^3/N -

w is the weight loss measured in grams,

p density of the worn material in g/mm^3 and

F is the applied load in N.

L Sliding Distance in m

The experimentation is performed on the EN 31 disc rotating at a maximum speed of 500, 1500 & 2000 rpm with the various loads of 50 N, 100 N, 150 N, and 200 N. The results we got from the experimentation is as plotted below in the form of table.

4. EXPERIMENTAL WEAR CALCULATION.

4.1 Specific Wear Rate Calculation.

4.1.1 with (Al94% Sic3% Gr3%) Variation of wear with load (N)

Sr. No.	Speed	Load	Time	wear Δm	Sliding Velocity (V)	Sliding Distance	Specific wear rate
	Rpm	N	Sec	gm.	m/sec	m	mm^3/Nm
1	500	50	600	0.0194	1.5708	942.45	1.519E-04
2	500	100	600	0.0754	1.5708	942.45	2.952E-04
3	500	150	600	0.1197	1.5708	942.45	3.124E-04
4	500	200	600	0.1758	1.5708	942.45	3.442E-04
5	1000	50	600	0.1089	3.1415	1884.9	4.264E-04
6	1000	100	600	0.2568	3.1415	1884.9	5.027E-04
7	1000	150	600	0.4965	3.1415	1884.9	6.480E-04
8	1000	200	600	0.6906	3.1415	1884.9	6.760E-04
9	1500	50	600	0.8690	4.7123	2827.35	2.268E-03
10	1500	100	600	1.8340	4.7123	2827.35	2.394E-03
11	1500	150	600	2.8556	4.7123	2827.35	2.485E-03
12	1500	200	600	4.1581	4.7123	2827.35	2.713E-03

Table 4: With (Al94% Sic3% Gr3%) Variation of wear with load (N)

4.1.2 With (Al88% Sic6% Gr6%) Variation of wear with load (N)

Sr. No.	Speed	Load	Time	wear Δm	Sliding Velocity (V)	Sliding Distance	Specific wear rate
	Rpm	N	Sec	gm.	m/sec	m	mm^3/Nm
1	500	50	600	0.0174	1.5708	942.45	1.363E-04
2	500	100	600	0.0670	1.5708	942.45	2.623E-04
3	500	150	600	0.1060	1.5708	942.45	2.767E-04
4	500	200	600	0.1701	1.5708	942.45	3.329E-04
5	1000	50	600	0.0930	3.1415	1884.9	3.642E-04
6	1000	100	600	0.2208	3.1415	1884.9	4.323E-04
7	1000	150	600	0.3865	3.1415	1884.9	5.044E-04
8	1000	200	600	0.5906	3.1415	1884.9	5.781E-04
9	1500	50	600	0.7540	4.7123	2827.35	1.968E-03
10	1500	100	600	1.6740	4.7123	2827.35	2.185E-03
11	1500	150	600	2.6320	4.7123	2827.35	2.290E-03
12	1500	200	600	3.8760	4.7123	2827.35	2.529E-03

Table 5: With (Al88% Sic6% Gr6%) Variation of wear with load (N)

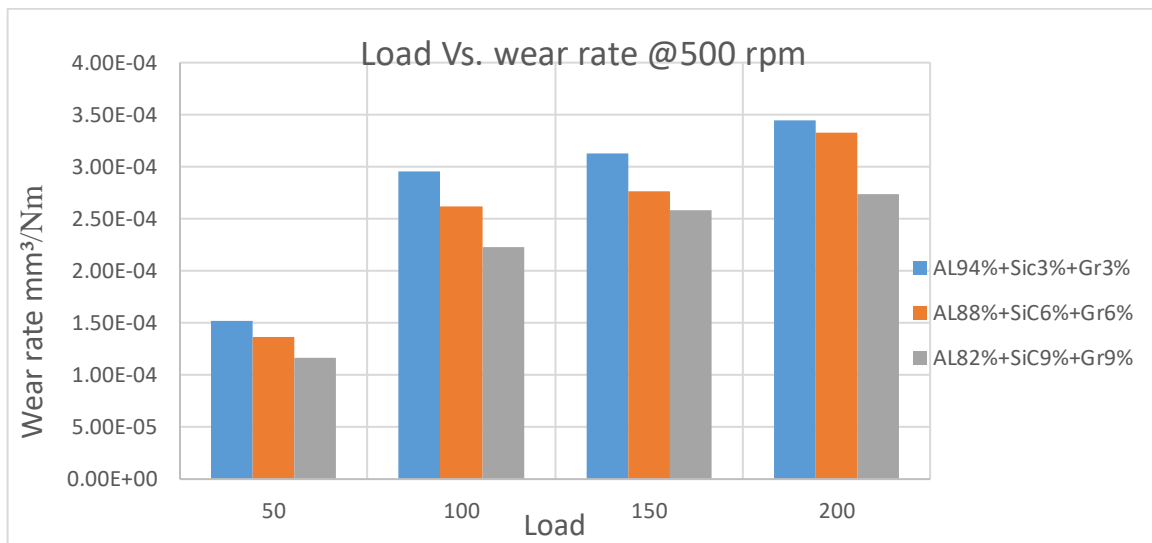
4.1.3 With (Al82% Sic9% Gr9%) Variation of wear with load (N)

Sr. No.	Speed	Load	Time	wear Δm	Sliding Velocity (V)	Sliding Distance	Specific wear rate
	Rpm	N	Sec	gm.	m/sec	m	mm ³ /Nm
1	500	50	600	0.0149	1.5708	942.45	1.167E-04
2	500	100	600	0.0570	1.5708	942.45	2.232E-04
3	500	150	600	0.0990	1.5708	942.45	2.584E-04
4	500	200	600	0.1400	1.5708	942.45	2.741E-04
5	1000	50	600	0.0840	3.1415	1884.9	3.290E-04
6	1000	100	600	0.2018	3.1415	1884.9	3.951E-04
7	1000	150	600	0.3265	3.1415	1884.9	4.261E-04
8	1000	200	600	0.4806	3.1415	1884.9	4.704E-04
9	1500	50	600	0.6740	4.7123	2827.35	1.759E-03
10	1500	100	600	1.4138	4.7123	2827.35	1.845E-03
11	1500	150	600	2.2340	4.7123	2827.35	1.944E-03
12	1500	200	600	3.1086	4.7123	2827.35	2.029E-03

Table 6: With (Al82% Sic9% Gr9%) Variation of wear with load (N)

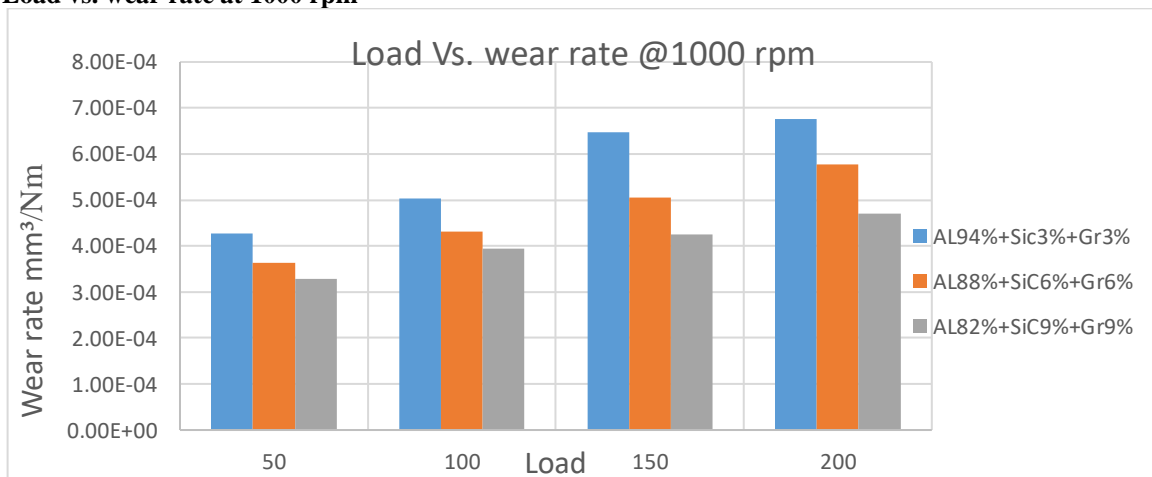
4.2 Graphical Comparison of specific wear rate.

4.2.1 Load vs. wear rate at 500 rpm



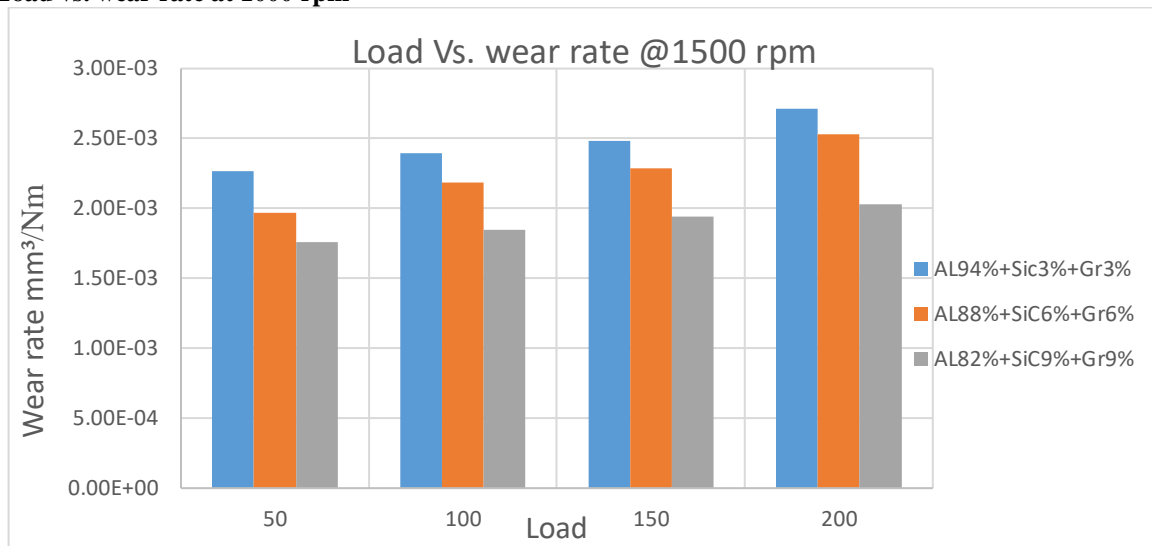
Graph 1: Load vs. Wear rate at 500 rpm

4.2.2 Load vs. wear rate at 1000 rpm



Graph 2: Load vs. Wear rate at 1000 rpm

4.2.2 Load vs. wear rate at 1000 rpm



Graph 3: Load vs. Wear rate at 1500 rpm

5 ANALYSIS OF RESULTS AND DISCUSSION BY USING RSM METHODOLOGY

5.1 RSM Experimental Design & Analysis

Response Surface Methodology, RSM (also known as **Response Surface Modeling**) is a technique to optimize the response(s) when two or more quantitative factors are involved. The dependent variables are known as responses, and the independent variables or factors are primarily known as the predictor variables in response surface methodology. While p-values are used for a particular point such as to test the hypothesis of “whether the 70-degree Fahrenheit is the most comfortable temperature or not,” the response surface is useful in determining a range of temperatures for the same comfort level. As maintaining the temperature exactly at a 70-degree could be very expensive, maintaining the temperatures within a range is often desired for cost-effective solution. Moreover, keeping very cool in summer or very hot in winter would be very wasteful. Response Surface Methodology, RSM, is very useful to optimize variables/factors more practically as compared to just the statistical significance test for a particular point (point estimate is the statistical jargon). Minitab 19 Software is used for RSM.

5.2 Components of Experimental Design

Consider the following diagram of a cake-baking process. There are three aspects of the process that are analyzed by a designed experiment:

- **Factors**, or inputs to the process. Factors can be classified as either controllable or uncontrollable variables. In this case, the controllable factors are the ingredients for the cake and the oven that the cake is baked in. The controllable variables will be referred to throughout the material as factors. Note that the ingredients list was shortened for this example - there could be many other ingredients that have a significant bearing on the end result (oil, water, flavoring, etc). Likewise, there could be other types of factors, such as the mixing method or tools, the sequence of mixing, or even the people involved. People are generally considered a Noise Factor (see the glossary) - an uncontrollable factor that causes variability under normal operating conditions, but we can control it during the experiment using blocking and randomization. Potential factors can be categorized using the Fishbone Chart (Cause & Effect Diagram) available from the Toolbox.
- **Levels**, or settings of each factor in the study. Examples include the oven temperature setting and the particular amounts of sugar, flour, and eggs chosen for evaluation.
- **Response**, or output of the experiment. In the case of cake baking, the taste, consistency, and appearance of the cake are measurable outcomes potentially influenced by the factors and their respective levels. Experimenters often desire to avoid optimizing the process for one response at the expense of another. For this reason, important outcomes are measured and analyzed to determine the factors and their settings that will provide the best overall outcome for the critical-to-quality characteristics - both measurable variables and assessable attributes.

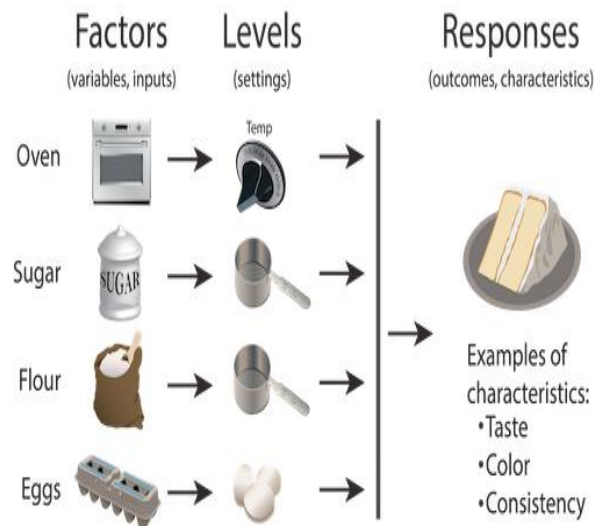


Fig 5: Factors, Level & Response

5.3 Experimental Result of wear Test on (Al 94% SiC3% Gr3%) by using RSM Methodology

Load (N)	Speed (RPM)	Time (sec)	Wear (mm ³ /Nm)	StdOrder	RunOrder	Blocks	PtType
50	500	600	1.519E-04	1	1	1	1
100	500	600	2.952E-04	2	2	1	1
150	500	600	3.124E-04	3	3	1	1
200	500	600	3.442E-04	4	4	1	1
50	1000	600	4.264E-04	5	5	1	1
100	1000	600	5.027E-04	6	6	1	1
150	1000	600	6.480E-04	7	7	1	1
200	1000	600	6.760E-04	8	8	1	1
50	1500	600	2.268E-03	9	9	1	1
100	1500	600	2.394E-03	10	10	1	1
150	1500	600	2.485E-03	11	11	1	1
200	1500	600	2.713E-03	12	12	1	1

Table 7: wear test on (Al94% SiC3% Gr3%) by RSM

5.3.1 Response Surface Regression: Wear (mm³/Nm) versus Load (N), Speed (RPM), (Al 94% SiC3% Gr3%)

1. Coded Coefficients

Term	Coef	SE Coef	T-Value	P-Value	VIF
Constant	0.000569	0.000026	21.79	0.000	
Load (N)	0.000146	0.000016	8.88	0.000	1.00
Speed (RPM)	0.001095	0.000015	73.10	0.000	1.00
Load (N)*Load (N)	-0.000011	0.000028	-0.38	0.714	1.00
Speed (RPM)*Speed (RPM)	0.000807	0.000026	31.12	0.000	1.00
Load (N)*Speed (RPM)	0.000062	0.000020	3.11	0.021	1.00

2. Model Summary

S	R-sq	R-sq(adj)	R-sq(pred)
0.0000424	99.91%	99.83%	99.46%

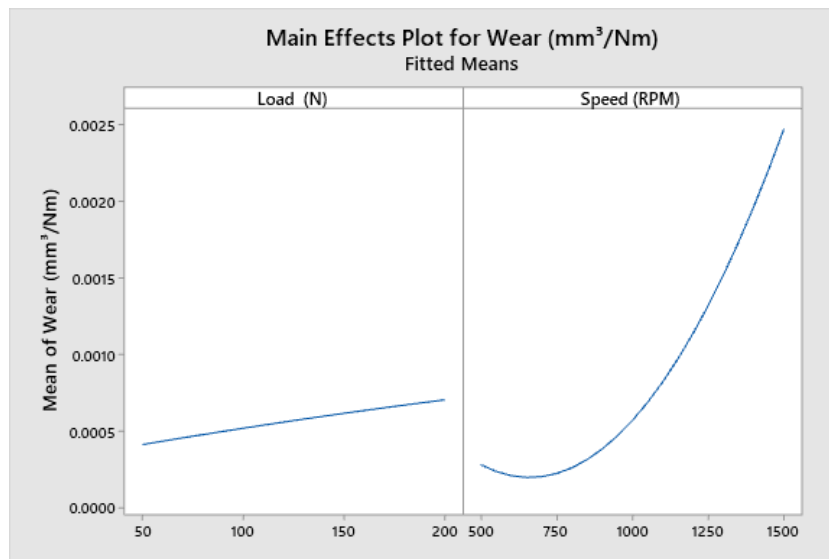
3. Analysis of Variance

Source	DF	Adj SS	Adj MS	F-Value	P-Value
Model	5	0.000011	0.000002	1280.12	0.000
Linear	2	0.000010	0.000005	2711.07	0.000
Load (N)	1	0.000000	0.000000	78.92	0.000
Speed (RPM)	1	0.000010	0.000010	5343.21	0.000
Square	2	0.000002	0.000001	484.41	0.000
Load (N)*Load (N)	1	0.000000	0.000000	0.15	0.714
Speed (RPM)*Speed (RPM)	1	0.000002	0.000002	968.67	0.000
2-Way Interaction	1	0.000000	0.000000	9.66	0.021
Load (N)*Speed (RPM)	1	0.000000	0.000000	9.66	0.021
Error	6	0.000000	0.000000		
Total	11	0.000011			

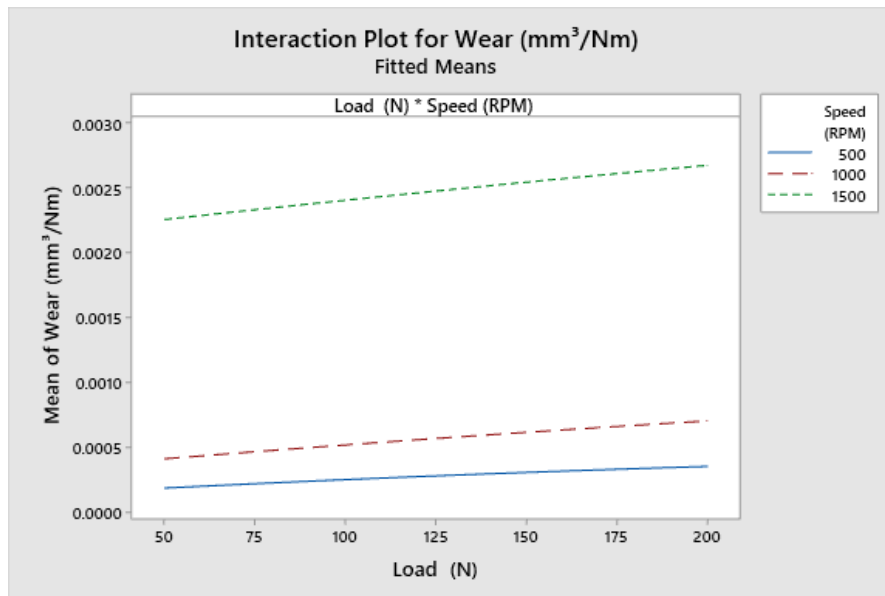
4. Regression Equation in Uncoded Units

$$\begin{aligned} \text{Wear (mm}^3/\text{Nm)} = & 0.001545 + 0.000001 \text{ Load (N)} - 0.000004 \text{ Speed (RPM)} \\ & - 0.000000 \text{ Load (N)*Load (N)} + 0.000000 \text{ Speed (RPM)*Speed (RPM)} \\ & + 0.000000 \text{ Load (N)*Speed (RPM)} \end{aligned}$$

5.3.2 Factorial Plots for Wear (mm³/Nm), (AL 93% Sic 3% Gr3%)

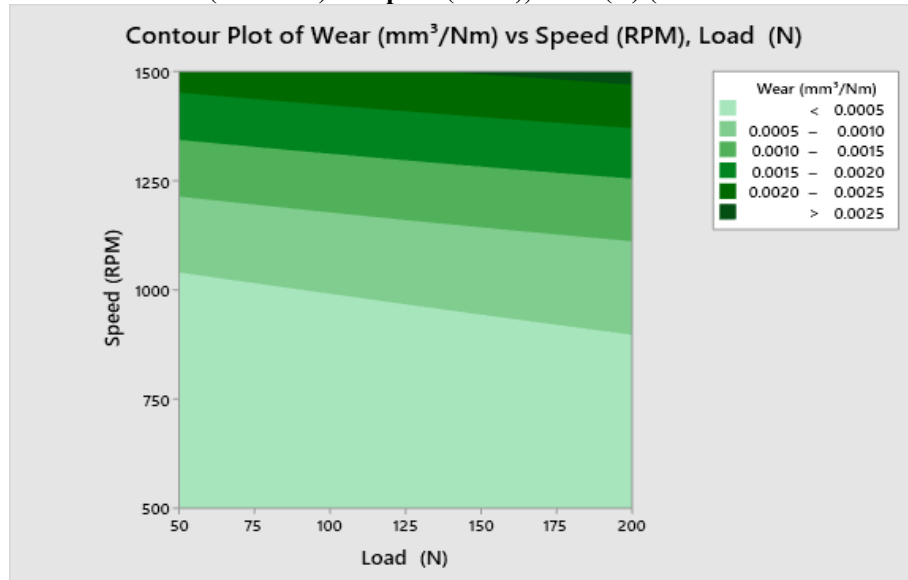


Graph 4: Main effects plot for wear (Al 94% Sic3% Gr3%)



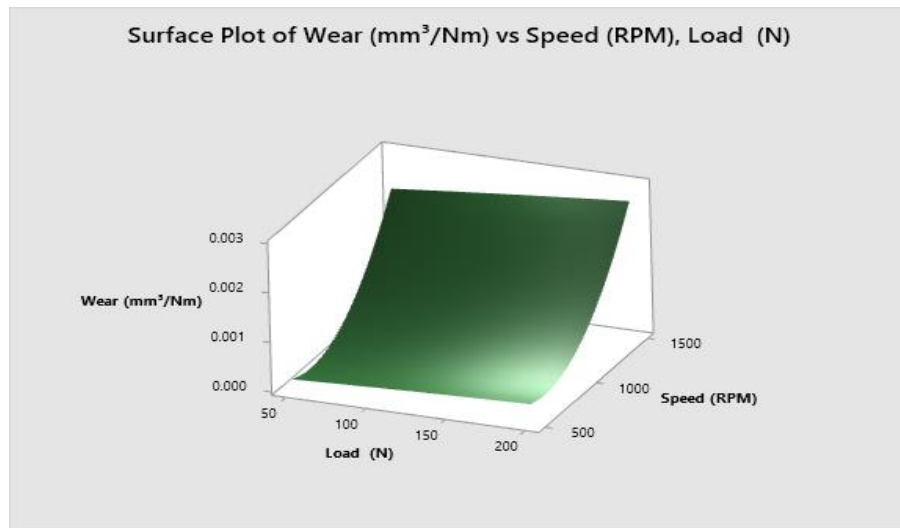
Graph 5: Interaction plot for wear (AL 94% Sic3% Gr3%)

5.3.3 Contour Plot of Wear (mm^3/Nm) vs. Speed (RPM), Load (N) (AL 94% Sic 3% Gr3%)



Graph 6: Contour Plot of Wear (mm^3/Nm) vs. Speed (RPM), Load (N) (AL 94% Sic 3% Gr3%)

5.3.4 Surface Plot of Wear (mm^3/Nm) vs. Speed (RPM), Load (N) (AL 94% Sic 3% Gr3%)



Graph 7: Surface Plot of Wear (mm^3/Nm) vs. Speed (RPM), Load (N) (AL 93% Sic 3% Gr3%)

5.4 Experimental Result of wear Test on (Al88% SiC6% Gr6%) by using RSM Methodology

Load (N)	Speed (RPM)	Time (sec)	Wear (mm^3/Nm)	StdOrder	RunOrder	Blocks	PtType
50	500	600	1.363E-04	1	1	1	1
100	500	600	2.623E-04	2	2	1	1
150	500	600	2.767E-04	3	3	1	1
200	500	600	3.329E-04	4	4	1	1
50	1000	600	3.642E-04	5	5	1	1
100	1000	600	4.323E-04	6	6	1	1
150	1000	600	5.044E-04	7	7	1	1
200	1000	600	5.781E-04	8	8	1	1
50	1500	600	1.968E-03	9	9	1	1
100	1500	600	2.185E-03	10	10	1	1
150	1500	600	2.290E-03	11	11	1	1
200	1500	600	2.529E-03	12	12	1	1

Table 8: wear test on (Al88% SiC6% Gr6%) by RSM

5.4.1 Response Surface Regression: Wear (mm^3/Nm) versus Load (N), Speed (RPM), (Al 88% SiC6% Gr6%)

1. Coded Coefficients

Term	Coef	SE Coef	T-Value	P-Value	VIF
Constant	0.000474	0.000029	16.41	0.000	
Load (N)	0.000155	0.000018	8.56	0.000	1.00
Speed (RPM)	0.000996	0.000017	60.09	0.000	1.00
Load (N)*Load (N)	-0.000008	0.000030	-0.26	0.806	1.00
Speed (RPM)*Speed (RPM)	0.000778	0.000029	27.11	0.000	1.00
Load (N)*Speed (RPM)	0.000089	0.000022	4.00	0.007	1.00

2. Model Summary

S	R-sq	R-sq(adj)	R-sq(pred)
0.0000469	99.86%	99.75%	99.10%

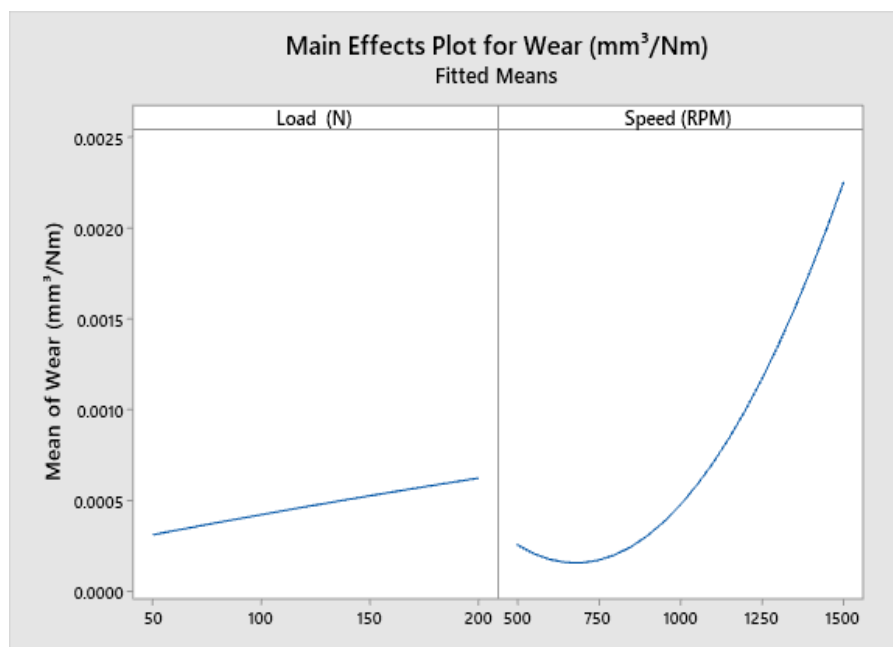
3. Analysis of Variance

Source	DF	Adj SS	Adj MS	F-Value	P-Value
Model	5	0.000010	0.000002	887.04	0.000
Linear	2	0.000008	0.000004	1842.19	0.000
Load (N)	1	0.000000	0.000000	73.28	0.000
Speed (RPM)	1	0.000008	0.000008	3611.11	0.000
Square	2	0.000002	0.000001	367.43	0.000
Load (N)*Load (N)	1	0.000000	0.000000	0.07	0.806
Speed (RPM)*Speed (RPM)	1	0.000002	0.000002	734.79	0.000
2-Way Interaction	1	0.000000	0.000000	15.98	0.007
Load (N)*Speed (RPM)	1	0.000000	0.000000	15.98	0.007
Error	6	0.000000	0.000000		
Total	11	0.000010			

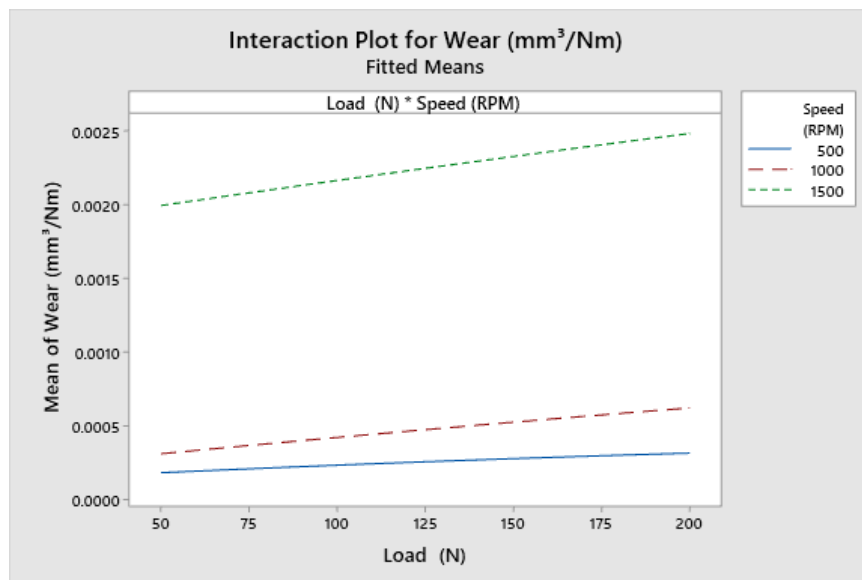
4. Regression Equation in Uncoded Units

$$\text{Wear (mm}^3\text{/Nm)} = 0.001610 + 0.000000 \text{ Load (N)} - 0.000005 \text{ Speed (RPM)} \\ - 0.000000 \text{ Load (N)*Load (N)} + 0.000000 \text{ Speed (RPM)*Speed (RPM)} \\ + 0.000000 \text{ Load (N)*Speed (RPM)}$$

5.4.2 Factorial Plots for Wear (mm³/Nm) (Al 88% SiC6% Gr6%)

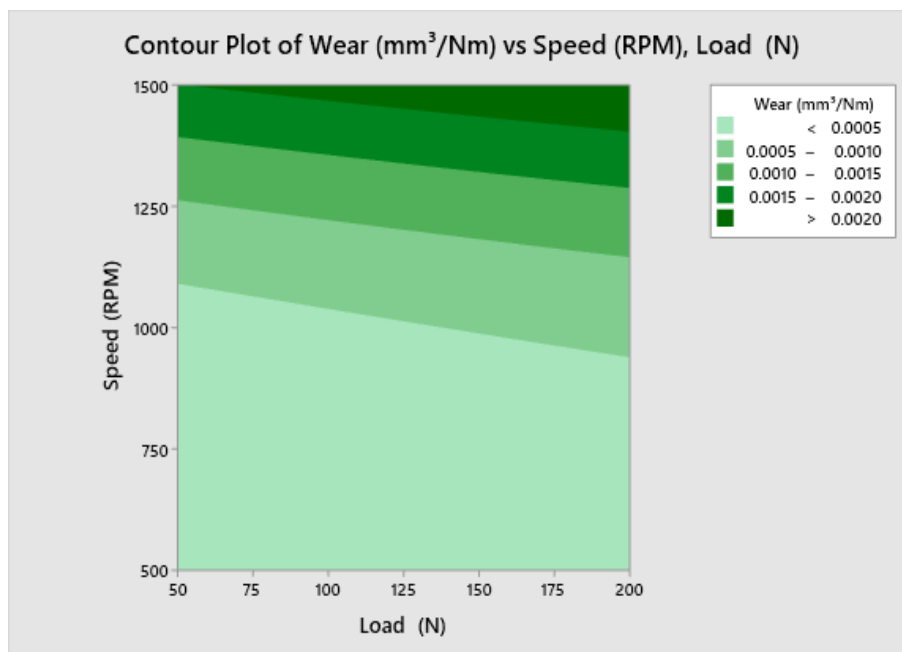


Graph 8: Main effects plots for wear (AL88% SiC6% Gr6%)



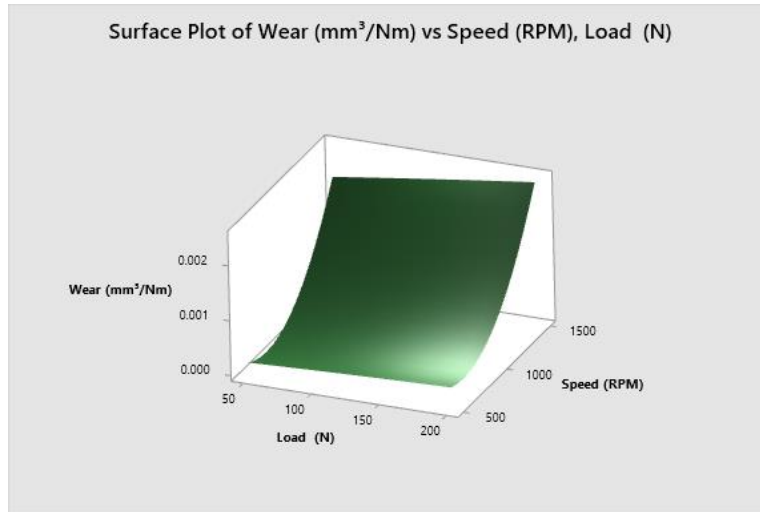
Graph 9: Interaction plot for wear (AL88% SiC6% Gr6%)

5.4.3 Contour Plot of Wear (mm^3/Nm) vs. Speed (RPM), Load (N) (Al 88% SiC6% Gr6%)



Graph 10: Counter plots for wear (AL88% SiC6% Gr6%)

5.4.4 Surface Plot of Wear (mm^3/Nm) vs. Speed (RPM), Load (N) (Al 88% SiC6% Gr6%)



Graph 11: Surface plots for wear (AL88% SiC6% Gr6%)

5.5 Experimental Result of wear Test on (Al82% SiC9% Gr9%) by using RSM Methodology

Load (N)	Speed (RPM)	Time (sec)	Wear (mm^3/Nm)	StdOrder	RunOrder	Blocks	PtType
50	500	600	1.167E-04	1	1	1	1
100	500	600	2.232E-04	2	2	1	1
150	500	600	2.584E-04	3	3	1	1
200	500	600	2.741E-04	4	4	1	1
50	1000	600	3.290E-04	5	5	1	1
100	1000	600	3.951E-04	6	6	1	1
150	1000	600	4.261E-04	7	7	1	1
200	1000	600	4.704E-04	8	8	1	1
50	1500	600	1.759E-03	9	9	1	1
100	1500	600	1.845E-03	10	10	1	1
150	1500	600	1.944E-03	11	11	1	1
200	1500	600	2.029E-03	12	12	1	1

Table 9: wear test on (Al82% SiC9% Gr9%) by RSM

5.5.1 Response Surface Regression: Wear (mm^3/Nm) versus Load (N), Speed (RPM) (Al82% SiC9% Gr9%)

1. Coded Coefficients

Term	Coef	SE Coef	T-Value	P-Value	VIF
Constant	0.000417	0.000015	28.01	0.000	
Load (N)	0.000093	0.000009	9.99	0.000	1.00
Speed (RPM)	0.000838	0.000009	98.16	0.000	1.00
Load (N)*Load (N)	-0.000021	0.000016	-1.36	0.223	1.00
Speed (RPM)*Speed (RPM)	0.000651	0.000015	44.02	0.000	1.00
Load (N)*Speed (RPM)	0.000030	0.000011	2.61	0.040	1.00

2. Model Summary

S	R-sq	R-sq(adj)	R-sq(pred)
0.0000241	99.95%	99.91%	99.69%

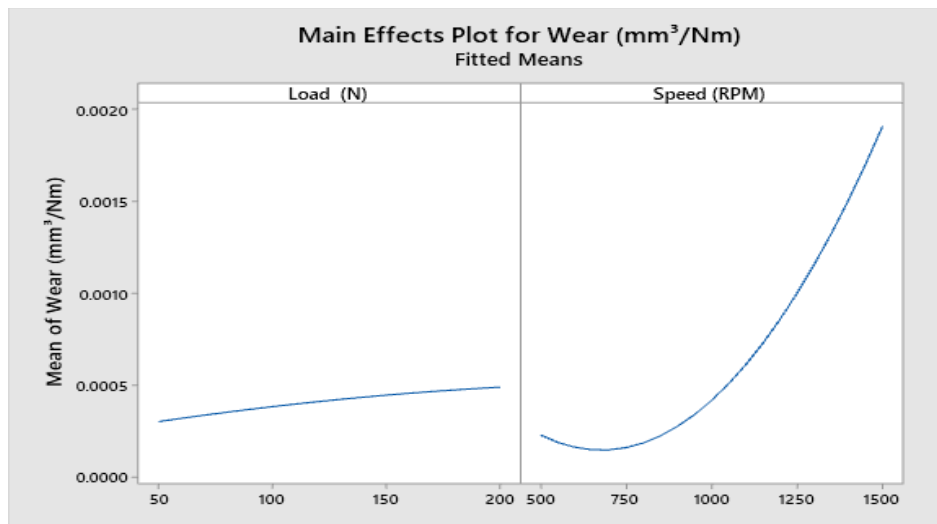
3. Analysis of Variance

Source	DF	Adj SS	Adj MS	F-Value	P-Value
Model	5	0.000007	0.000001	2336.50	0.000
Linear	2	0.000006	0.000003	4867.88	0.000
Load (N)	1	0.000000	0.000000	99.86	0.000
Speed (RPM)	1	0.000006	0.000006	9635.90	0.000
Square	2	0.000001	0.000001	969.97	0.000
Load (N)*Load (N)	1	0.000000	0.000000	1.85	0.223
Speed (RPM)*Speed (RPM)	1	0.000001	0.000001	1938.09	0.000
2-Way Interaction	1	0.000000	0.000000	6.82	0.040
Load (N)*Speed (RPM)	1	0.000000	0.000000	6.82	0.040
Error	6	0.000000	0.000000		
Total	11	0.000007			

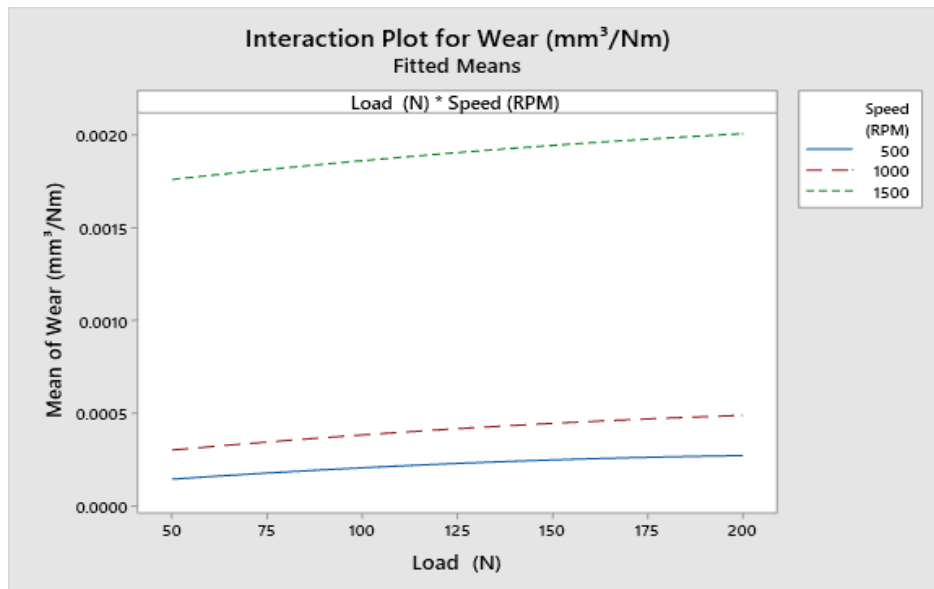
4. Regression Equation in Uncoded Units

$$\begin{aligned} \text{Wear (mm}^3/\text{Nm)} = & 0.001230 + 0.000001 \text{ Load (N)} - 0.000004 \text{ Speed (RPM)} \\ & - 0.000000 \text{ Load (N)*Load (N)} \\ & + 0.000000 \text{ Speed (RPM)*Speed (RPM)} \\ & + 0.000000 \text{ Load (N)*Speed (RPM)} \end{aligned}$$

5.5.2 Factorial Plots for Wear (mm³/Nm) (Al82% SiC6% Gr6%)

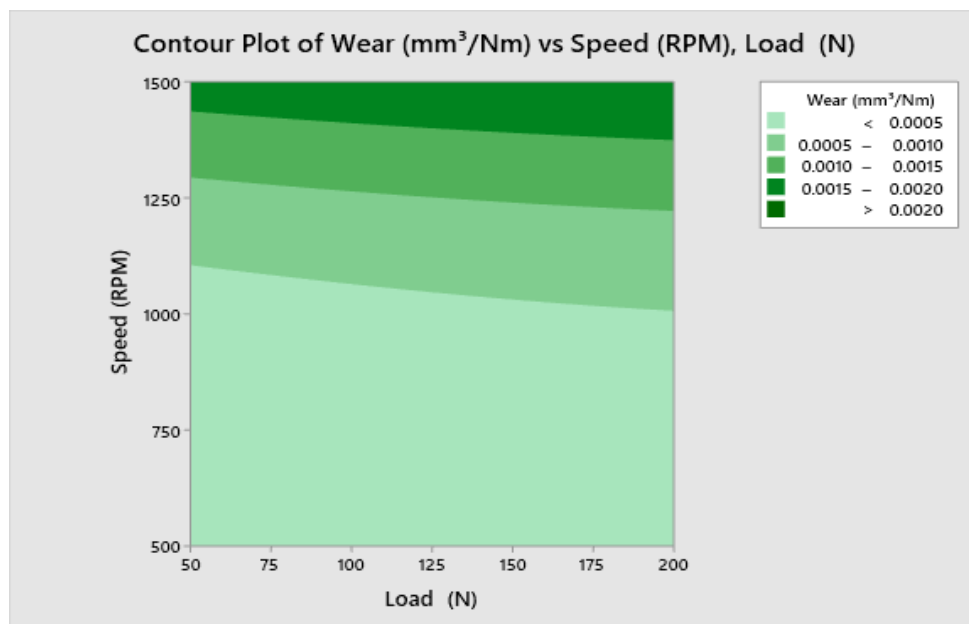


Graph 12: Main Effects plot for wear (AL82% SiC9% Gr9%)



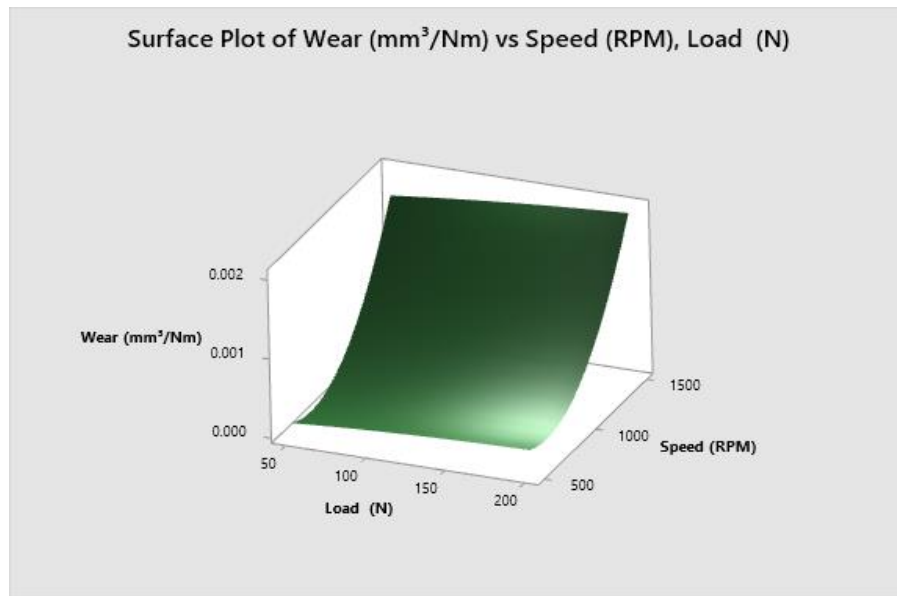
Graph 13: Interaction plot for wear (AL82% Sic9% Gr9%)

5.5.3 Contour Plot of Wear (mm^3/Nm) vs. Speed (RPM), Load (N) (AL82% SiC6% Gr6%)



Graph 14: Counter plot for wear (AL82% Sic9% Gr9%)

5.5.4 Surface Plot of Wear (mm^3/Nm) vs. Speed (RPM), Load (N) (Al82% SiC6% Gr6%)



Graph 15: Surface plot for wear vs. Speed, Load (Al82% SiC9% Gr9%)

CONCLUSION

1. Aluminium alloy & its composite SiC, graphite have been effectively fabricated by stir casting method using two step addition of particles in the melt.
2. Al6061, SiC & Graphite composites were shown uniform distribution of reinforcement particles in the base matrix material.
3. The wear resistance of Al6061 alloy increased after addition of SiC & Graphite particle. The Volumetric wear loss affected by load & Sliding speed.
4. Wear loss decrease with increase in percentage of SiC & Graphite composite. I.e. Addition of SiC 9Vol% and Gr 9Vol% to Al6061 decrease the Specific wear rate.
5. The hardness, ultimate tensile strength as well as percentage of elongation reduce with increase in SiC & Graphite content.
6. Hardness increases with increase in wt % of SiC & Gr
7. Tensile Strength, Yield Strength and % Elongation increases with increase in wt % of SiC & Gr upto 15 %
8. From the results, the use of steel particles as replacement of conventional reinforcements such as SiC & Gr in AMCs, has great promise for applications where high specific strength, toughness and wear resistance are desired in service.
9. The hardness of the composites increased approximately by 15% with increase in steel particles from 3 to 9 wt.% of SiC & Gr; also, for the same range of steel concentration, the ultimate tensile strength increased with increase in steel wt.% and were all higher than that of 9 wt.% reinforced SiC & Gr. The specific strength and fracture toughness equally followed the same trend with respect to steel concentration, and comparison with SiC & Gr reinforced composite composition

REFERENCES

1. Kenneth Kanayo Alaneme, Adetomilola Victoria Fajemisin, Nthabiseng Beauty Maledi Development of aluminium-based composites reinforced with steel and graphite particles: structural, mechanical and wear characterization. Received 2 November 2017 Accepted 30 April 2018
2. Pardeep Sharmaa, Krishan Paliwal, Ramesh Kumar Garg, Satpal Sharmac, Dinesh Khanduja A study on wear behaviour of Al/6101/graphite composites, Received 13 October 2016 Received in revised form 22 December 2016 Accepted 26 December 2016 Available online 7 January 2017.
3. Nagara M1, Auradi, Parashivamurthy and Kori a Comparative Study on Wear Behavior of Al6061-6% sic and Al6061- 6% Graphite Composites, Nagaral, J Appl Mech Eng 2016.

4. Siddabathula Madhusudan, Mohammed Moulana Mohiuddin Sarcar b, Narsipalli Bhargava Rama Mohan Rao Mechanical properties of Aluminum-Copper(p) composite metallic materials, 2016
5. Navnath Sambhaji Kalyankar, Rahul D. Shelke study of properties of Al-25/SiC metal matrix composite fabricated by using stir casting method International Journal of Mechanical Engineering and Technology (IJMET) Volume 7, Issue 5, September–October 2016, pp.133–141, Article ID: IJMET_07_05_016.
6. Md. Habibur Rahmana, H. M. Mamun Al Rashed, Characterization of silicon carbide reinforced aluminum matrix composites, 2013
7. Pardeep Sharma, Dinesh Khanduja, Satpal Sharma, Parametric Study of Dry Sliding Wear of Aluminium Metal Matrix Composites by Response Surface Methodology, 4th International Conference on Materials Processing and Characterization, 2015.
8. Viney Kumara, Rahul Dev Guptab N K Batra Comparison of Mechanical Properties and effect of sliding velocity on wear properties of Al 6061, Mg 4%, Fly ash and Al 6061, Mg 4%, Graphite 4%, Fly ash Hybrid Metal matrix composite. 3rd International Conference on Materials Processing and Characterization (ICMPC 2014).
9. S. C. Patnaik, P. K. Swain, P. K. Mallik, S. K. Sahoo Wear Characteristics of Aluminium-Graphite Composites Produced by Stir Casting Technique, ISSN: 2231-3818 (online), ISSN: 2321-4236 (print) Volume 4, Issue 3.
10. Ricardo Augusto Gonçalves and Márcio Bacci da Silva Influence of Copper Content on 6351 Aluminum Alloy Machinability
11. R. L. Deuis, C. Subramanian & J. M. Yellup dry sliding wear of aluminium composites-a review (Received 25 February 1996 revised 30 August 1996; accepted 14 October 1996).
12. M. S. Prabhudeva, V. Auradib, K. Venkateswarluc N. H. Siddalingaswamyd and S. A. Kori Influence of Cu Addition on Dry Sliding Wear Behavior of A356 Alloy. 12th global congress on manufacturing and management, 2014
13. Mechanical properties of aluminium metal matrix composites under impact loading. Hamouda and M.S.J. Hashrni
14. Palanisamy Shanmugasundaram Investigation on the Wear Behaviour of Eutectic Al-Si Alloy– Al₂O₃ - Graphite Composites Fabricated Through Squeeze Casting. Received: December 7, 2013; Revised: May 11, 2014
15. Devaraju Aruri, Kumar Adepu, Kumaraswamy Adepu, Kotiveerachari Bazavada Wear and mechanical properties of 6061-T6 aluminum alloy surface hybrid composites [(SiC+ Gr) and (SiC+ Al₂O₃)] fabricated by friction stir processing
16. Michael Oluwatosin Bodunrin, Kenneth Kanayo Alaneme, Lesley Heath Chown Aluminium matrix hybrid composites: a review of reinforcement philosophies; mechanical, corrosion and tribological characteristics. Received 6 September 2014 Accepted 5 May 2015 Available online 9 June 2015.
17. Wear properties of brass samples subjected to constrained groove pressing process M. Ebrahimi, Sh. Attarilar, F. Djavanroodi, C. Gode, H.S. Kim,
18. Adel Mahmood Hassan, Sulieman Z.S. Al-Dhi Improvement in the wear resistance of brass components by the ball burnishing process, Received 22 March 1998
19. Monika Walkowicz, Impact of oxidation of copper and its alloys in laboratory-simulated conditions on their antimicrobial efficiency.
20. Mechanical properties of aluminium metal matrix composites under impact loading.
21. Leaching and recovery of zinc and copper from brass slag by sulfuric acid I.M. Ahmed, A.A. Nayl, J.A. Daoud
22. Salim Ahy n, Nilay Y ksel, H lya Durmu, Simge Gen alp, WEAR BEHAVIOR OF Al/SiC/GRAPHITE AND Al/FeB/GRAPHITE HYBRID COMPOSITES.
23. Z. B. Luklinska and J. E. Castle, microstructural study of initial corrosion product of aluminium-brass alloy after exposure to natural seawater, 1983
24. Performance of aluminium alloy graphite bearings in a diesel engine B.P. Krishnan, N. Raman, K. Narayanaswamy and P.K. Rohatgi
25. HIROSHI TOKISUE, Friction and Wear Properties of Aluminum-Particulate Graphite Composites, 1977.
26. Wear characteristics of metals T. S. Eyre
27. Fabrication methods used to prepare Al metal matrix composites- A review **Prem Shankar Sahu, R. Banchhor**
28. V. K. Dodiya J. P. Parmar, a Study of Various Wear Mechanism and its Reduction Method, 2016